



Research Article

Ginsenoside Rb1 attenuates methamphetamine (METH)-induced neurotoxicity through the NR2B/ERK/CREB/BDNF signalings *in vitro* and *in vivo* models



Genmeng Yang^{a, b, 1}, Juan Li^c, Yanxia Peng^{a, b}, Baoyu Shen^{a, b}, Yuanyuan Li^{a, b}, Liu Liu^{a, b}, Chan Wang^{a, b}, Yue Xu^{a, b}, Shucheng Lin^{a, b}, Shuwei Zhang^{a, b}, Yi Tan^{a, b}, Huijie Zhang^{a, b}, Xiaofeng Zeng^{a, b, *}, Qi Li^{d, **}, Gang Lu^{e, ***}

^a NHC Key Laboratory of Drug Addiction Medicine, Kunming Medical University, Kunming, Yunnan Province, China

^b School of Forensic Medicine, Kunming Medical University, Kunming, Yunnan Province, China

^c School of Basic Medicine, Kunming Medical University, Kunming, Yunnan Province, China

^d SDIVF R&D Centre, Hong Kong, China

^e CUHK-SDU Joint Laboratory on Reproductive Genetics, School of Biomedical Sciences, the Chinese University of Hong Kong, Hong Kong, China

ARTICLE INFO

Article history:

Received 31 March 2021

Received in revised form

9 July 2021

Accepted 9 July 2021

Available online 14 July 2021

Keywords:

Methamphetamine

Ginsenoside Rb1

SH-SY5Y cells

Conditioned place preference

NR2B

ERK

CREB

BDNF

ABSTRACT

Aim: This study investigates the effects of ginsenoside Rb1 (GsRb1) on methamphetamine (METH)-induced toxicity in SH-SY5Y neuroblastoma cells and METH-induced conditioned place preference (CPP) in adult Sprague-Dawley rats. It also examines whether GsRb1 can regulate these effects through the NR2B/ERK/CREB/BDNF signaling pathways.

Methods: SH-SY5Y cells were pretreated with GsRb1 (20 μ M and 40 μ M) for 1 h, followed by METH treatment (2 mM) for 24 h. Rats were treated with METH (2 mg/kg) or saline on alternating days for 10 days to allow CPP to be examined. GsRb1 (5, 10, and 20 mg/kg) was injected intraperitoneally 1 h before METH or saline. Western blot was used to examine the protein expression of NR2B, ERK, p-ERK, CREB, p-CREB, and BDNF in the SH-SY5Y cells and the rats' hippocampus, nucleus accumbens (NAc), and prefrontal cortex (PFC).

Results: METH dose-dependently reduced the viability of SH-SY5Y cells. Pretreatment of cells with 40 μ M of GsRb1 increased cell viability and reduced the expression of METH-induced NR2B, p-ERK, p-CREB and BDNF. GsRb1 also attenuated the expression of METH CPP in a dose-dependent manner in rats. Further, GsRb1 dose-dependently reduced the expression of METH-induced NR2B, p-ERK, p-CREB, and BDNF in the PFC, hippocampus, and Nac of rats.

Conclusion: GsRb1 regulated METH-induced neurotoxicity *in vitro* and METH-induced CPP through the NR2B/ERK/CREB/BDNF regulatory pathway. GsRb1 could be a therapeutic target for treating METH-induced neurotoxicity or METH addiction.

© 2021 The Korean Society of Ginseng. Publishing services by Elsevier B.V. This is an open access article under the CC BY-NC-ND license (<http://creativecommons.org/licenses/by-nc-nd/4.0/>).

1. Introduction

Methamphetamine (METH) is widely used as a recreational drug. Long-term consumption of METH elicits somatic, psychiatric,

* Corresponding author. School of Forensic Medicine, Kunming Medical University, 650500, 1168 West Chunrong Road, Yuhua Avenue Chenggong District, Kunming, Yunnan, China.

** Corresponding author.

*** Corresponding author.

E-mail addresses: zxf2004033@163.com (X. Zeng), liqihku@gmail.com (Q. Li), lugang@cuhk.edu.hk (G. Lu).

¹ Genmeng YANG, Juan LI, and Yanxia PENG contributed equally to this work.

and cognitive impairment [1,2]. METH abuse has increased dramatically in recent years, becoming a serious public health problem worldwide [2]. Current treatments are of minimal efficacy, so there is an urgent need to develop novel pharmacotherapies to combat METH dependence [3].

As a psychostimulant, METH can increase the extracellular level of dopamine (DA) in the nervous system by promoting DA release and attenuating DA reuptake [4]. We reported that the co-administration of ketamine and alcohol alters dopamine-related gene expression and BDNF in the cortical-striatal circuitry [5]. Mesocorticolimbic signaling inhibits the availability of ventral

striatal D2-type receptors and promotes impulsivity in METH-dependent individuals [6]. This rewarding circuitry involves the nucleus accumbens (NAc) and its afferents from the medial prefrontal cortex (mPFC); the NAc also receives dopaminergic and glutamatergic afferents from the hippocampal formation [7].

The present study focuses on corticolimbic circuits, which are comprised of the PFC, NAc, and hippocampus. Except for DA, the roles of other neurotransmitters and their respective receptors—including glutamate, γ -Aminobutyric acid (GABA), and serotonin—in the motivational effects of METH have been identified [2,8–10]. Recent studies have shown that METH affects synaptic glutamatergic activity by elevating the level of NR2B-containing N-methyl-D-aspartate receptors in the PFC [11]. METH can also modulate cytokine production, such as interleukin-6 and tumor necrosis factor- α , through the cAMP/PKA/CREB/ERK signaling pathways [12]. However, the mechanisms of NR2B alteration in corticolimbic circuits induced by METH dependence are not yet fully understood.

The conditioned place preference (CPP) paradigm has been used to study the reinforcement properties of drugs, such as amphetamine, METH, cocaine, and morphine [13]. CPP has been developed to identify small molecules that carry therapeutic value to treat drug abuse [13]. METH-induced drug-seeking (i.e., CPP) and drug-taking (i.e., self-administration) behaviors are mediated, at least in part, through D1/D5 receptors in the dorsal hippocampus [14]. Acute administration of METH induces locomotor stimulation through the activation of the NR2B receptor [15]. A recent experiment demonstrated that YQA14, a selective D3 receptor antagonist, can attenuate METH-induced CPP in rodents [16].

Ginsenoside Rb1 (GsRb1), a key constituent of ginseng, is widely used in the pharmacological examination of the effects of ginseng. GsRb1's chemical structures are shown in Fig. 2B. GsRb1 has a variety of neuroprotective effects on the brain, such as the attenuation of excitotoxicity, neuroinflammation, and oxidative stress; the maintenance of neurotransmitter balance; the inhibition of autophagy; and anti-tau phosphorylation [17–19]. Recent work in our laboratory has demonstrated that GsRb1 protects the blood–brain barrier (BBB) against the neurotoxicity exerted by the HIV-1 Tat (human immunodeficiency virus-1 trans-activator of transcription protein) and METH in rats [20]. Previous studies have suggested that GsRb1 may modulate METH-induced CPP in mice through the regulation of DA receptors [21]. No works to date have examined whether GsRb1 can mediate the effects of METH on NR2B-containing NMDARs and CPP. To address this knowledge gap, we tested the hypothesis that GsRb1 attenuates METH-induced drug-seeking behaviors by regulating the NR2B/ERK/CREB/BDNF signaling pathways in the corticolimbic circuit.

First, we investigated the pharmacological effects of METH and GsRb1 on dopaminergic neurons using SH-SY5Y human neuroblastoma cells. Through this process, we assessed the mechanisms of the NR2B/ERK/CREB/BDNF signaling pathway underlying these effects. We also performed *in vivo* CPP tests to determine whether GsRb1 can mediate drug-seeking behaviors induced by chronic METH administration in SD rats. We then further explored whether NR2B/ERK/CREB/BDNF signaling is involved in METH-induced neurotoxicity and drug-seeking behavior and GsRb1 rescue effects.

2. Materials and methods

2.1. Chemicals and reagents

METH (purity 100%) was dissolved in saline (pH 7) (National Institutes for Food and Drug Control, China). GsRb1 (purity 98%) was sourced from Chengdu Must Biotechnology Co. Ltd. (China). The antibodies against NR2B, ERK, p-ERK, CREB, p-CREB, BDNF, and

β -actin were sourced from Cell Signaling Technology (USA), and HRP-conjugated secondary antibodies were obtained from Sigma (Germany).

2.2. Cell lines and cell culture

Human neuroblastoma SH-SY5Y cells sourced from the National Infrastructure of Cell Line Resource (NICR, China) were grown in Dulbecco's Modified Eagle Medium (DMEM/F12) (1:1) medium containing 15% FBS at 37°C incubators with 5% CO₂.

2.3. Cell viability assay

Cell Counting Kit-8 was used to determine cell viability (Beyotime, China). SH-SY5Y cells were cultured in a 96-well plate at a density of 2×10^4 /100 μ l and treated with varying concentrations of METH and Rb1 for 24 h. We then added 10 μ l of a CCK-8 solution to each well and incubated the cells for 1 to 2 h. Mean optical density (OD, absorbance at 450 nm) was used to calculate the percentage of viability: cell viability percentage = $(OD_{\text{treatment}} - OD_{\text{blank}}) / (OD_{\text{control}} - OD_{\text{blank}}) \times 100\%$ (see Fig. 1: Supplementary Information).

2.4. *In vitro* experimental design

For the drug treatment, the cells were pretreated with Rb1 (20 μ M and 40 μ M) for 1 h [22–24] and 2 mM METH treatment for 24 h [25], when the cells were at the confluence of 75 to 85%. The cells were then rinsed twice with phosphate-buffered saline (PBS) before the drug treatment. For the *in vitro* experiment, cells were randomly grouped as follows: (I) vehicle group; (II) METH (2 mM) treatment group; (III) Rb1 (40 μ M mM) treatment group; (IV) Rb1 (20 μ M) pretreatment + METH (2 mM) treatment group; and (V) Rb1 (40 μ M) pretreatment + METH (2 mM) treatment group.

2.5. *In vivo* animal experiments

2.5.1. Animals

Male adult Sprague-Dawley (SD) rats were sourced from Kunming Medical University (China). The rats were kept in an environmentally controlled room ($23 \pm 2^\circ\text{C}$) under a standard 12 h:12 h light/dark cycle. The experimental procedures were approved by the Institutional Animal Care and Use Committee of Kunming Medical University.

2.5.2. Experimental design

Male SD rats ($n = 60$) were equally and randomly divided into six groups. Drug dosages were based on those of previous studies [20,24]: (1) control rats received 0.9% saline through intraperitoneal (IP) injection of 10 ml/kg; (2) METH (2 mg/kg, IP) treatment; (3) Rb1 (20 mg/kg, IP) treatment; (4) Rb1 (5 mg/kg, IP) pretreatment 1 h + METH (2 mg/kg, IP) treatment; (5) Rb1 (10 mg/kg) pretreatment 1 h + METH (2 mg/kg) treatment; and (6) Rb1 (20 mg/kg) pretreatment 1 h + METH (2 mg/kg).

2.5.3. CPP experiment

2.5.3.1. Apparatus. The apparatus used for CPP had two equal-sized chambers made of plexiglass with different colors and textures (35 cm \times 35 cm \times 35 cm) (XR-XT401, Xinruan Information Technology Co. Ltd., Shanghai, China). The internal spaces between the two chambers were separated by a central tunnel 15 cm (L) \times 35 cm (W/H). The central tunnel was gray, with a featureless floor. Per previous studies, the CPP experiment was conducted in three distinct phases: habituation, conditioning, and post-conditioning [26].

2.5.3.2. CPP model. Habituation phase (days 1–3): On days 1–3, each rat was housed in the CPP chambers and could freely explore the chambers for 30 min to minimize stress and initial bias. Pre-conditioning test was videotaped for 15 min on day 3 (see Fig. 2A). Rats were excluded when they exhibited a preference to any chamber for >67% of the total time [27].

Conditioning phase (days 4–13): Each rat received an IP administration of either 2 mg/kg METH or 10 ml/kg saline on alternating days. On days 4, 6, 8, 10, and 12, the rats were administered METH and confined to one compartment of the apparatus. They were given saline injections and confined in the other chamber on days 5, 7, 9, 11, and 13. Each rat's locomotor activity was videotaped for 30 min daily for 10 days (5 drug sessions and 5 saline sessions) (see Fig. 2A). Naive animals received a vehicle (saline 10 ml/kg) or Rb1 (5, 10, 20 mg/kg, IP) 1 h before each METH or saline administration during the conditioning phase. All drugs were freshly prepared every day before injection.

Post-conditioning phase (day 14): CPP was evaluated again 24 h after the final administration. Drug treatment was not performed on the test day. The rats were again placed in the central tunnel and allowed free access to both chambers for 15 min. Any changes in place preference (CPP scores) were determined by determining the difference between the time spent in the saline-paired compartment and the METH-paired compartment of the apparatus [16]. Preference behavior was determined by determining the difference

between the time spent in the METH- and saline-conditioned chambers in the pre- and post-conditioning phases.

All rats were euthanized 24 h after the last test. Each rat's PFC, hippocampus, and NAC were harvested and frozen for subsequent analysis.

2.6. Western blot analysis

Western blotting was carried out as previously described [25]. Briefly, the cells and brain tissues were homogenized in a protein extraction buffer (Beyotime, China). BCA protein assay was used to determine protein concentration (Beyotime, China). They were incubated overnight with primary antibodies (anti-NR2B, anti-ERK, anti-p-ERK, anti-CREB, anti-p-CREB, anti-BDNF, and anti-β-actin) at 4°C, followed by secondary antibodies for 2 h at ambient temperature. The films were captured using the ECL chemiluminescence system. Protein bands were quantified using ImageJ software (Version 1.46).

2.7. Statistical analysis

The western blot and CPP results were assessed using a one-way ANOVA. Results are reported as mean ± SEM. Pearson correlation was applied to analyze the relationship between METH-induced CPP behavior and protein expression levels in the brain. Analyses

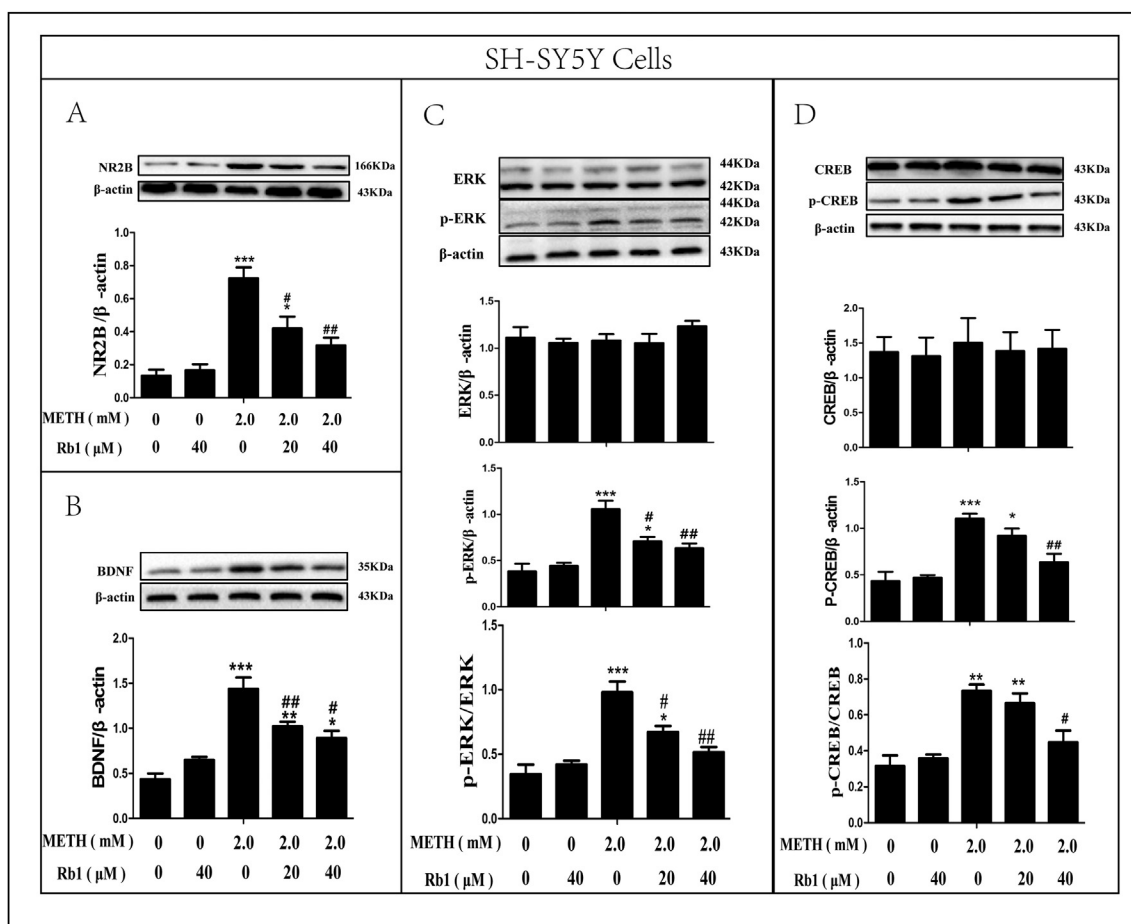


Fig. 1. The effects of METH and Rb1 on the expressions of NR2B, ERK, p-ERK, pERK/ERK, CREB, p-CREB, p-CREB/CREB, and BDNF in METH-induced SH-SY5Y cells. The expression levels of NR2B (A), BDNF (B), ERK, p-ERK, p-ERK/ERK (C), and p-CREB, p-CREB/CREB (D) were analyzed by western blot. (**p < 0.01,***p < 0.001, indicating a significant difference compared with the control group; #p < 0.05,##p < 0.01,###p < 0.001, indicating a significant difference compared with the METH group, n = 3–5 per group). Data are presented as mean ± SEM in at least 3 experiments.

were performed using SPSS 9.0 and GraphPad Prism (version 5.0). $p < 0.05$ indicates statistical significance.

3. Results

3.1. Cell viability assay

Cell viability was reduced with an increase in METH concentrations from 0.5 mM to 3 mM. As low as 0.1 mM METH reduced cell viability, and the effect was most obvious with 2 mM METH. This indicates that METH reduces the viability of SH-SY5Y cells dose-dependently. Pretreatment with 40 μ M Rb1 increased cell viability, indicating that Rb1 provides a neuroprotective effect against METH-induced cytotoxicity (see Fig. 1: Supplementary Information).

3.2. Rb1 reduces the elevated expression of NR2B, p-ERK, p-ERK/ERK, p-CREB, p-CREB/CREB, and BDNF in METH-treated SH-SY5Y cells

The expression of NR2B, p-ERK, p-ERK/ERK, p-CREB, p-CREB/CREB and BDNF increased significantly in the METH group [NR2B: $F(14) = 20.1, p < 0.0001$; p-ERK: $F(14) = 307, p < 0.0001$; p-ERK/ERK: $F(14) = 94.56, p < 0.0001$; p-CREB: $F(14) = 23.77, p < 0.0001$; p-CREB/CREB: $F(14) = 6.41, p = 0.008$; BDNF: $F(14) = 21.84, p < 0.0001$] without altering the total ERK and CREB expression. When cells were pretreated with Rb1 (20, 40 μ M) for 1 h, the expression of NR2B, p-ERK, p-ERK/ERK, and BDNF gradually decreased in the Rb1 (20, 40 μ M) groups, and p-CREB and p-CREB/CREB decreased in the Rb1 (40 μ M) group (Fig. 1). The results

indicate that METH can elevate the protein expression levels of NR2B, p-ERK, p-ERK/ERK, p-CREB, p-CREB/CREB and BDNF, and the pretreatment of Rb1 can reverse the process.

3.3. Rb1 attenuates METH-induced CPP in rats

CPP is considered an effective method for measuring drug-induced reward effects. The experimental schedule applied in the present study is presented in Fig. 2A. Compared with the pre-conditioning phase, the rats stayed longer in the drug-paired chamber of the apparatus after they were treated with METH, as shown in Fig. 2B. However, after the rats were treated with Rb1 (5, 10, or 20 mg/kg), the differences between pre- and post-conditioning gradually decreased. These results indicate that Rb1 can attenuate METH-induced CPP, as shown in Fig. 2C.

3.4. Effect of Rb1 and METH on the expression of NR2B, ERK, p-ERK, p-ERK/ERK, CREB, p-CREB, p-CREB/CREB, and BDNF in PFCs

Compared to the saline group, the protein expression of NR2B, p-ERK, p-ERK/ERK, p-CREB, p-CREB/CREB, and BDNF increased significantly in PFCs without altering their total CREB and ERK expression after being treated with METH. Prior treatment with Rb1 (5, 10, or 20 mg/kg) caused the expression levels of NR2B and p-CREB to decrease significantly in the Rb1 (20 mg/kg) + METH group, and BDNF, p-ERK, p-ERK/ERK, and p-CREB/CREB decreased by varying degrees in the Rb1 (10, 20 mg/kg) + METH group. The protein expression was not statistically significant in the Rb1 (5 mg/kg) + METH group. [NR2B: $F(17) = 9.284, p = 0.0008$; p-ERK: $F(17) = 14.59, p < 0.0001$; p-ERK/ERK: $F(17) = 12.23, p = 0.0002$; p-

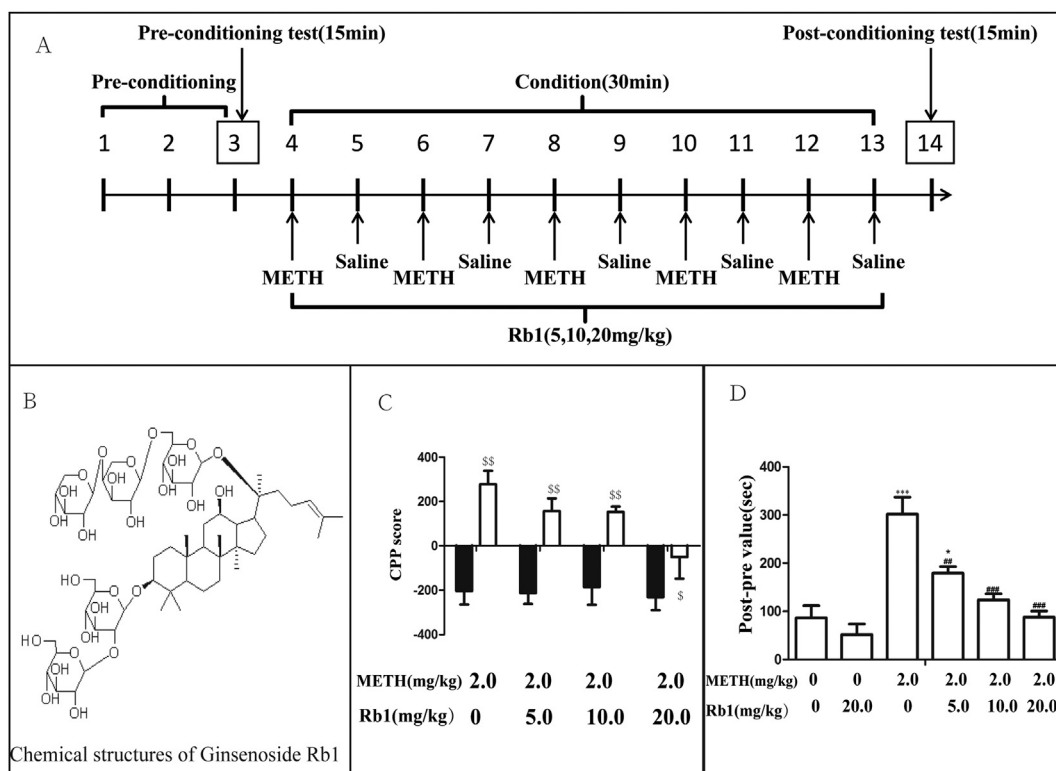


Fig. 2. Effect of Rb1 on METH-induced CPP in rats. (A) The experimental protocol for Rb1 and METH treatments, rats received METH (2 mg/kg IP) or saline (10 ml/kg IP) injections 1 h after Rb1 (5, 10, 20 mg/kg, IP) or saline (10 ml/kg IP) treatments. (B) The CPP score was calculated by subtracting the time spent in the saline-paired compartment from the time spent in the drug-paired compartment. CPP scores show that METH significantly increased the time spent on the drug-paired side ($p < 0.05, **p < 0.01$, indicating a significant difference compared with the pre-conditioning, $n = 10$). (C) Place preference data were expressed by subtracting the time spent in the saline-paired compartment from the time spent in the drug-paired compartment. Columns indicate mean \pm SEM ($*p < 0.05, **p < 0.01, ***p < 0.001$, indicating a significant difference compared with the control group; $##p < 0.01, ###p < 0.001$, indicating a significant difference compared with the METH group, $n = 10$).

CREB: $F(17) = 43.07, p < 0.0001$; p-CREB/CREB: $F(17) = 65.70, p < 0.0001$; BDNF: $F(17) = 83.02, p < 0.0001$]. These results are shown in Fig. 3.

3.5. Effect of Rb1 and METH on NR2B, ERK, p-ERK, p-ERK/ERK, CREB, p-CREB, p-CREB/CREB and BDNF in hippocampus

The expression of NR2B, p-ERK, p-ERK/ERK, p-CREB, p-CREB/CREB, and BDNF increased significantly in the METH group. Pretreatment with Rb1 resulted in a gradual decrease in the expression of NR2B, p-ERK, p-ERK/ERK, p-CREB/CREB, and BDNF in the Rb1 (10, 20 mg/kg) + METH groups. Further, p-CREB was significantly reduced in the Rb1 (20 mg/kg) + METH group. Alterations in the expressions of these proteins were not statistically significant in the Rb1 (5 mg/kg) + METH group. [NR2B: $F(17) = 7.986, p = 0.0016$; p-ERK: $F(17) = 1.016, p = 0.0005$; p-ERK/ERK: $F(17) = 2.057, p = 0.1421$; p-CREB: $F(17) = 15.81, p < 0.0001$; p-CREB/CREB: $F(17) = 6.090, p < 0.0049$; BDNF: $F(17) = 15.49, p < 0.0001$]. These results are shown in Fig. 4.

3.6. Effect of Rb1 and METH on NR2B, ERK, p-ERK, p-ERK/ERK, CREB, p-CREB, p-CREB/CREB and BDNF in NAC

Fig. 5 illustrates that the expression of NR2B, p-ERK, p-ERK/ERK, p-CREB, p-CREB/CREB, and BDNF increased significantly in the METH group compared to the saline group. Pretreatment of NAC

with increasing dose of Rb1 (5, 10, or 20 mg/kg) gradually, decreased the expression levels of NR2B, p-ERK, p-ERK/ERK, p-CREB, and p-CREB/CREB in the Rb1 (10, 20 mg/kg) + METH groups. BDNF decreased in the Rb1 (20 mg/kg) + METH group. Here too, changes in the expression of these proteins were not statistically significant in the Rb1 (5 mg/kg) + METH group. [NR2B: $F(17) = 73.52, p < 0.0001$; p-ERK: $F(17) = 45.31, p < 0.0001$; p-ERK/ERK: $F(17) = 11.41, p = 0.0003$; p-CREB: $F(17) = 31.59, p < 0.0001$; p-CREB/CREB: $F(17) = 6.964, p = 0.0029$; BDNF: $F(17) = 10.06, p = 0.0006$]. These results are shown in Fig. 5.

3.7. Correlation analysis between ex vivo protein expression and in vivo CPP measures

A Pearson analysis was performed to determine whether a correlation existed between drug-seeking behaviors and protein expression in the brain. Protein expressions were found to highly correlate with post-pre values in the METH group (A–D) (NR2B, $r = 0.924, p < 0.001, n = 9$; p-ERK, $r = 0.975, p < 0.001, n = 9$; p-CREB, $r = 0.972, p = 0.001, n = 9$; BDNF, $r = 0.927, p < 0.001, n = 9$). In the Rb1 + METH group, however, no correlation was established between drug-seeking behaviors and NR2B, p-ERK, p-CREB, or BDNF levels (A, B, C, D) (NR2B, $r = 0.515, p = 0.156, n = 9$; p-ERK, $r = 0.690, p = 0.40, n = 9$; p-CREB, $r = 0.051, p = 0.897, n = 9$; BDNF, $r = 0.047, p = 0.904, n = 9$). These results are shown in Fig. 6.

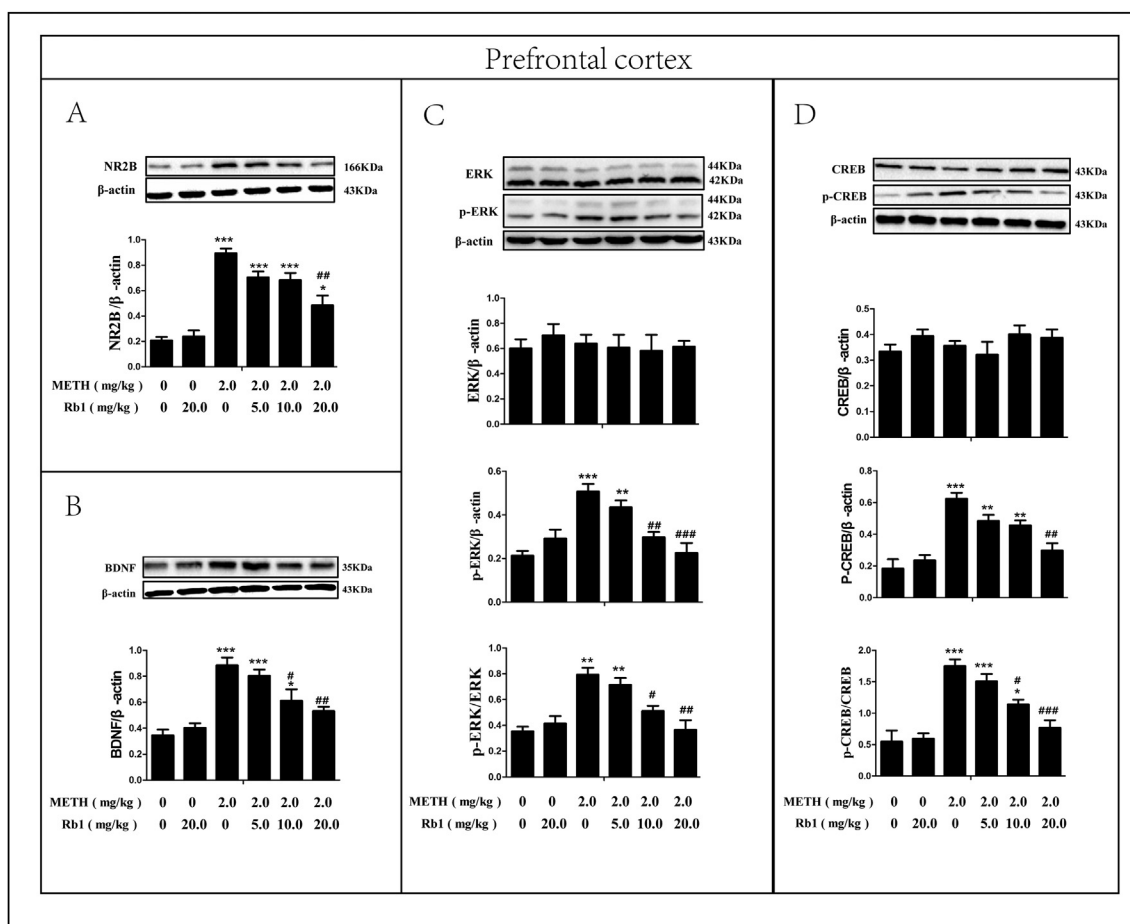


Fig. 3. Effects of Rb1 and METH on the expressions of NR2B, ERK, p-ERK, p-ERK/ERK, CREB, p-CREB, p-CREB/CREB, and BDNF in the PFC of METH-induced CPP rats. The expression levels of NR2B (A), BDNF (B), ERK, p-ERK, p-ERK/ERK (C), and p-CREB, p-CREB/CREB (D) were detected by western blot. (* $p < 0.05$, ** $p < 0.01$, *** $p < 0.001$, indicating a significant difference compared with the control group; # $p < 0.05$, ## $p < 0.01$, ### $p < 0.001$, indicating a significant difference compared with the METH group, $n = 3$). The data are represented as the means \pm SEMs of three independent experiments.

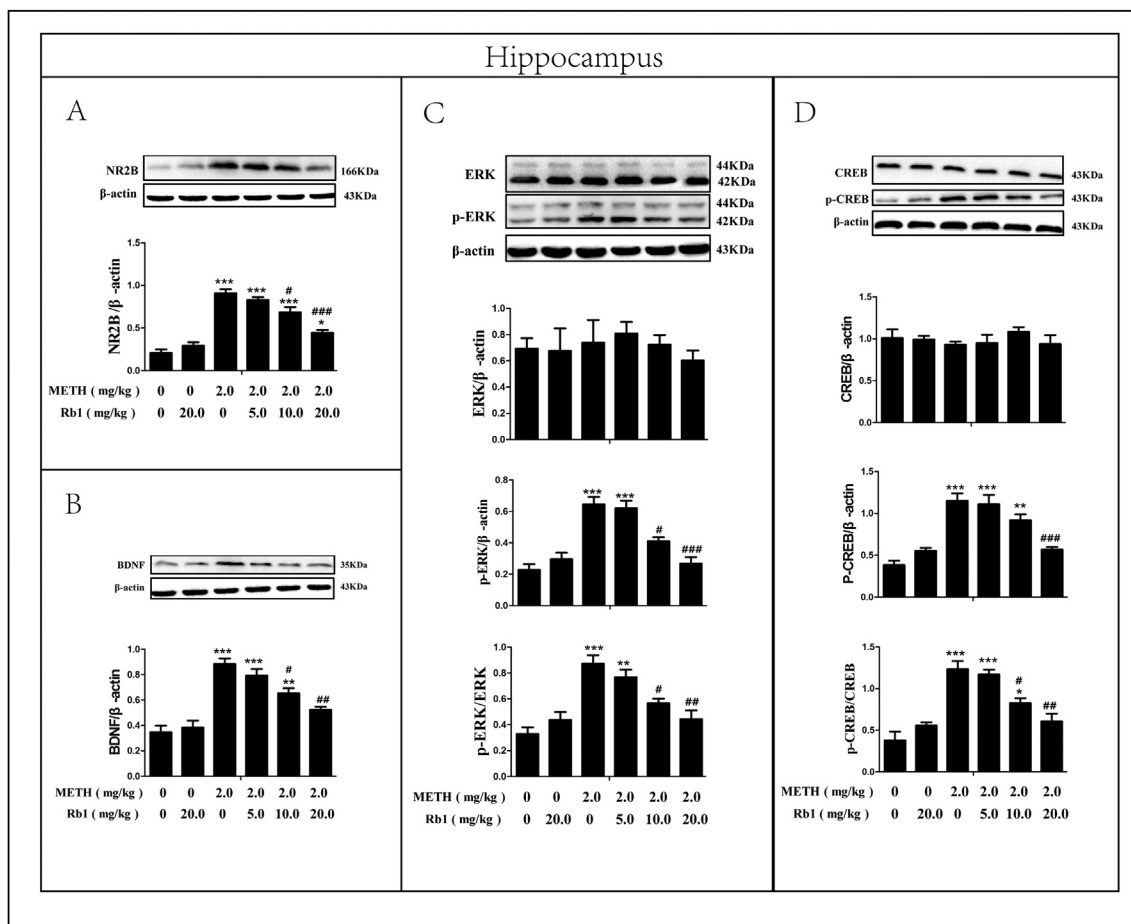


Fig. 4. Effects of Rb1 and METH on the expressions of NR2B, ERK, p-ERK, p-ERK/ERK, CREB, p-CREB, p-CREB/CREB, and BDNF in hippocampus of METH-induced CPP rats. The expression levels of NR2B (A), BDNF (B), ERK, p-ERK, p-ERK/ERK (C), and p-CREB, p-CREB/CREB (D) were detected by western blot. (*p < 0.05, **p < 0.01, ***p < 0.001, indicating a significant difference compared with the control group; #p < 0.05, ##p < 0.01, ###p < 0.001, indicating a significant difference compared with the METH group, n = 3). The data are represented as the means ± SEMs of three independent experiments.

4. Discussion

In this study, we spent 6 months observing the therapeutic effects of GsRb1 on METH-induced cytotoxicity in SH-SY5Y cells and METH-induced CPP changes in rats. CPP is commonly used to investigate drug-seeking behaviors. This study extended the field by successfully establishing a METH-induced place preference rat model. Previously, our research group demonstrated that METH-induced CPP elevated the protein kinase A (PKA)/CREB signaling pathway [28]. We found that repeated dosing of GsRb1 can attenuate METH-induced CPP. This supports prior findings by Kim et al (1996; 1998), who reported that ginseng extracts inhibit hyperactivity and CPP induced by METH. Unlike our study, Kim et al used high dosages of ginseng (e.g., 100 mg/kg). The GsRb1 used in our study showed dose-dependent effects on CPP. The highest dose of GsRb1, 20 mg/kg, had the greatest inhibition effects on the expression of METH-induced CPP.

According to our results, METH strongly upregulated the protein expression of NR2B in SH-SY5Y and the cortic limbic network *in vivo*. Pretreatment with GsRb1 (40 μM) was found to significantly downregulate the expression of NR2B induced by METH in SH-SY5Y *in vitro*. Consistent with these *in vitro* findings, heightened expression levels of NR2B were observed in the PFC, NAc, and hippocampus; pretreatment with GsRb1 reduced NR2B expression

in these brain areas *ex vivo*. In the PFC, pretreating with 20 mg/kg of GsRb1 downregulated NR2B levels compared to the METH-treated group. In the hippocampus, NR2B expression levels were reduced by pretreatments of 10 and 20 mg/kg of GsRb1. In the NAc, reduced NR2B was induced by pretreatments with 5, 10, and 20 mg/kg of GsRb1.

Our data and the work of previous studies demonstrate that GsRb1 affects areas of the brain differently. Li et al [15] reported that amphetamine and METH can increase NR2B levels in the midbrain in rats. Their study linked DA and glutamate neurotransmission to amphetamine and METH in the midbrain. NR2B is critical for many forms of synaptic plasticity [29], locomotor sensitization to drugs of abuse [30], and CPP in mice [31]. Further, increased NR2B can lead to an influx of calcium and excitotoxic damage of neurons [32]. Interestingly, GsRb1 selectively inhibits the activity of calcium channels in hippocampal neurons [33]. Another recent study showed that GsRb1 can directly inhibit basal NMDAR-mediated synaptic transmission [34]. Kim et al [35] reported that the calcium influx evoked by NMDAR activation could be mediated by ginseng Rg3. Thus, our study's observed inhibition of NR2B might contribute to the protective effect of GsRb1 by dampening the influx of calcium. Additional investigation is required to study whether the calcium channel in the

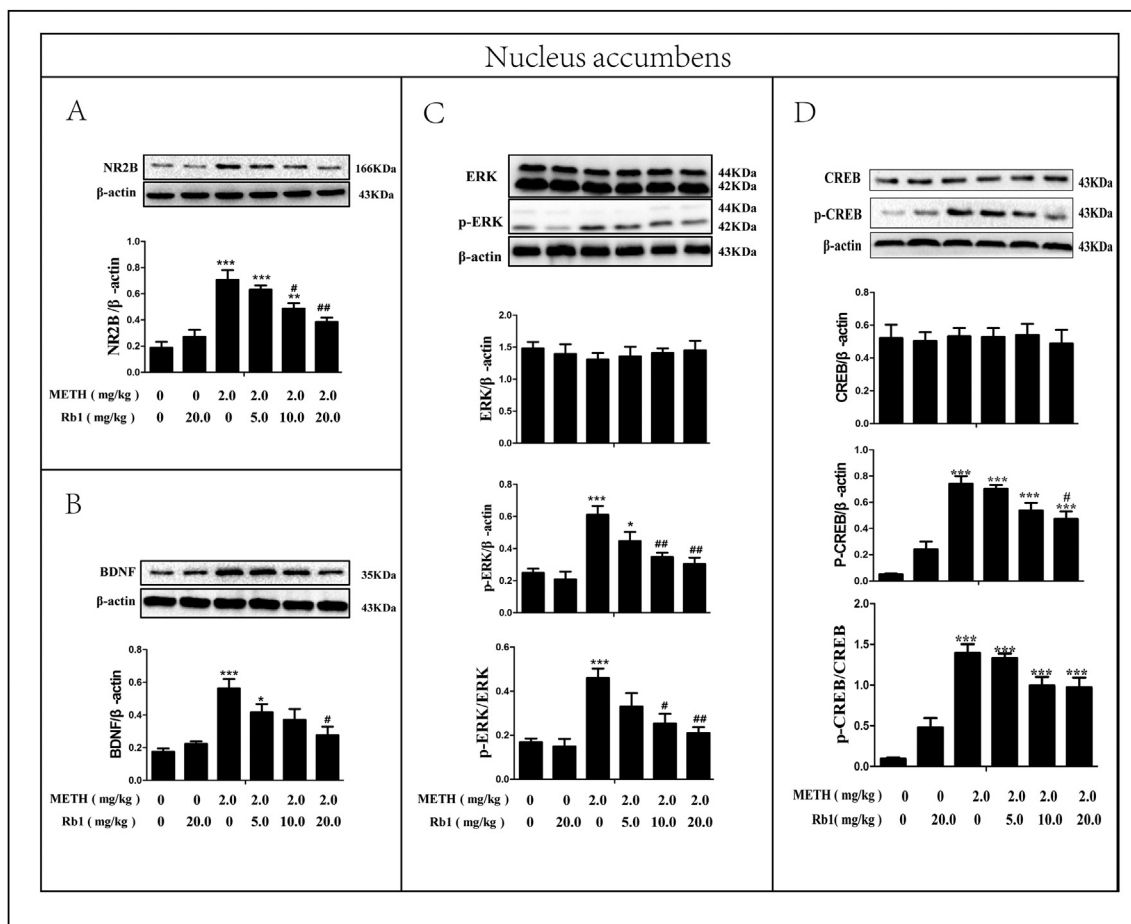


Fig. 5. Effects of Rb1 and METH on the expressions of NR2B, ERK, p-ERK, p-ERK/ERK, CREB, p-CREB, p-CREB/CREB, and BDNF in Nac of METH-induced CPP rats. The expression levels of NR2B (A), BDNF (B), ERK, p-ERK, p-ERK/ERK (C), and p-CREB, p-CREB/CREB (D) were detected by western blot. (*p < 0.05, **p < 0.01, ***p < 0.001, indicating a significant difference compared with the control group; #p < 0.05, ##p < 0.01, ###p < 0.001, indicating a significant difference compared with the METH group, n = 3). The data are represented as the means ± SEMs of three independent experiments.

glutamatergic synapse is involved in the neuroprotection of GsRb1 against chronic METH consumption.

ERK signaling involves both NMDAR-dependent synaptic plasticity and the control of transcription factor activity, such as Ras/ERK/CREB signaling [36]. As with the ERK-mediated phosphorylation of CREB at serine-133 via p90rsk [37,38], the phosphorylation of CREB occurs in response to Ca²⁺/calmodulin-dependent and stress-activated signaling pathways [39]. The transcription factor BDNF is modulated by Ca²⁺-induced CREB and the activation of CaM-dependent protein kinase II/IV [40]. Thus, CREB is a nuclear effector of the NR2B/ERK/CREB/BDNF signaling pathway. The p-CREB/BDNF is strongly associated with neuronal regeneration, development, survival, addiction, depression, and cognition [41,42]. Because CREB influences signaling information from multiple sources, it is not surprising that the enhancement of CREB functions affects many complex behaviors—some beneficial and others detrimental. Elevated neuronal functions of CREB could lead to drug tolerance and dependence [42,43]. Our data show that the phospho-ERK/CREB signaling cascade was upregulated in the corticolimbic brain circuits of rats after chronic exposure to METH and in the SH-SY5Y cell line. Previous studies have demonstrated that p-CREB levels increase in the ventral tegmental area (VTA) after long-term consumption of certain drugs [44,45]. Recent evidence has further shown that the activity of the NR2B/ERK/CREB signaling is vital for modulating reward-seeking behavior [46,47]. We found

that pretreatment with GsRb1 significantly downregulated the expression of p-ERK and p-CREB induced by METH in SH-SY5Y cells and CPP rats. We observed significant relationships between drug-seeking behaviors and NR2B/p-ERK/p-CREB/BDNF expression in the METH group. However, there were no correlations between protein expression and behaviors in the Rb1 treatment group. These data indicate that GsRb1 treatment might block the correlation between brain protein expression and behavior in rats.

Accumulating evidence suggests that BDNF plays a role in METH-induced neurotoxicity [48,49], drug reward responses, locomotor sensitization [50], and METH addiction and withdrawal [51]. Chronic METH exposure increases BDNF levels in the brain [49,52] and induces neuronal death, apoptosis [49,53], and hippocampal atrophy [54]. We observed that BDNF expression was elevated in SH-SY5Y cells and in the hippocampus, PFC, and Nac brain circuits after chronic exposure to METH. Recently, epigenetic mechanisms, particularly in exon IV of the BDNF gene, have been shown to be strongly associated with drug addiction and enhanced relapse vulnerability [55,56]. In our experiments, pretreatment with GsRb1 significantly downregulated the expression of BDNF induced by METH in SH-SY5Y and CPP rats. These data indicate that NR2B, p-ERK, p-CREB, and BDNF are involved in the protective effect of GsRb1 on METH-induced neurotoxicity in SH-SY5Y cells and CPP rats.

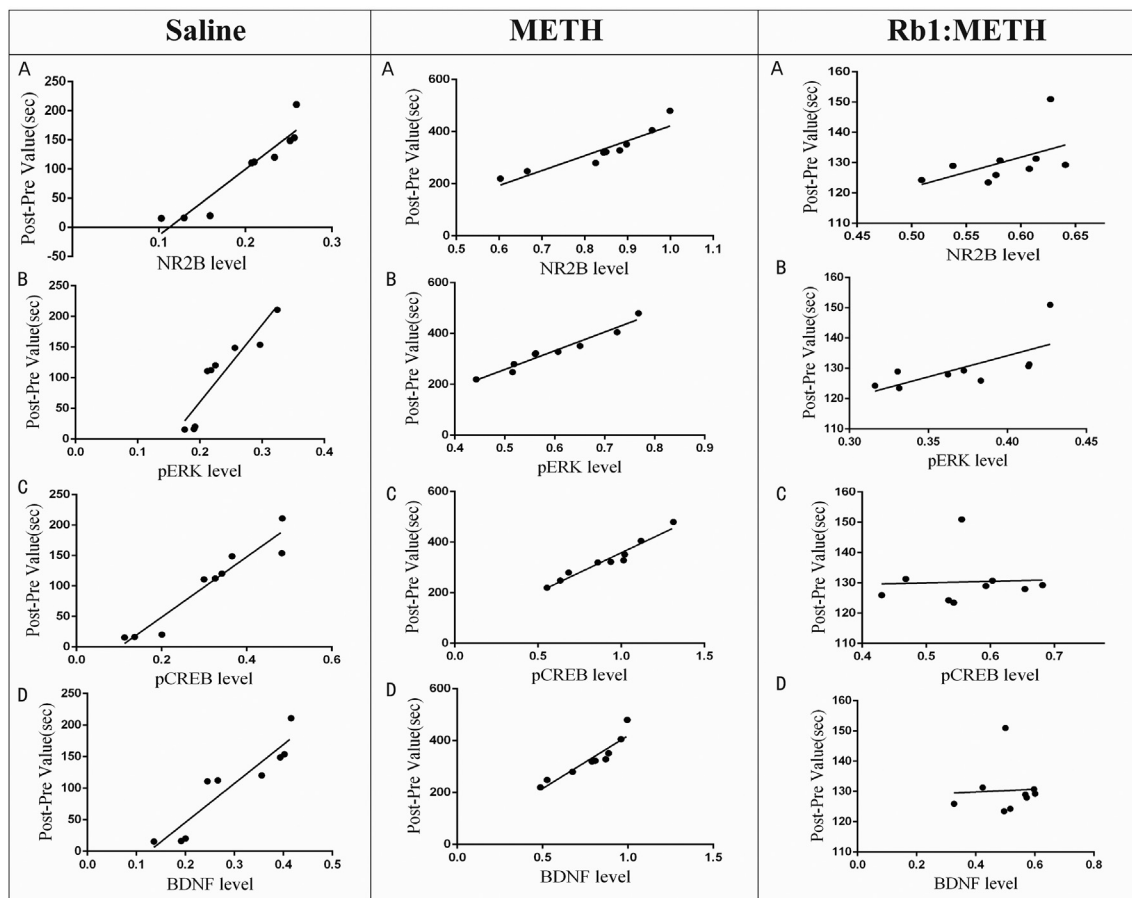


Fig. 6. NR2B, p-ERK, p-CREB, and BDNF expressions in the PFC, hippocampus and NAC correlate with preference ratios. NR2B (A), p-ERK (B), p-CREB (C), and BDNF (D) expressions significantly correlated with preference ratios in the PFC. (A) $r = 0.877$, $p < 0.01$; (B) $r = 0.914$, $p < 0.01$; (C) $r = 0.924$, $p < 0.001$; (D) $r = 0.866$, $p < 0.01$; $n = 9$. (A–D) NR2B (A), p-ERK (B), p-CREB (C), and BDNF (D) expression significantly correlated with preference ratios in the hippocampus. (A) $r = 0.961$, $p < 0.001$; (B) $r = 0.917$, $p < 0.01$; (C) $r = 0.918$, $p < 0.001$; (D) $r = 0.894$, $p < 0.01$; $n = 9$. NR2B (A), p-ERK (B), p-CREB (C), and BDNF (D) expression significantly correlated with preference ratios in the NAC. (A) $r = 0.936$, $p < 0.001$; (B) $r = 0.882$, $p < 0.01$; (C) $r = 0.931$, $p < 0.001$; (D) $r = 0.850$, $p < 0.01$; $n = 9$.

5. Conclusion

Our findings show that METH induces elevated levels of NR2B, p-ERK, p-CREB, and BDNF in SH-SY5Y cells and corticolimbic brain circuits in CPP rats. High dosages of GsRb1 can significantly reduce NR2B, p-ERK, p-CREB, and BDNF expression. This suggests that GsRb1 can dampen METH-induced toxicity in SY5Y cells and METH-induced drug-seeking behaviors in rats by downregulating the NR2B/ERK/CREB/BDNF signaling pathways. Thus, GsRb1 has potential as a therapeutic target for METH addiction or neurotoxicity.

Funding sources

This work was supported by the National Nature Science Foundation of China (81960340 and 82060382), the NHC Key Laboratory of Drug Addiction Medicine (2020DAMARA-008), the Basic Research Program of Yunnan Province (202001AT070098), and the Yunnan Applied Basic Research Projects Joint Special Project (202001AY070001-015).

Declaration of competing interest

The authors declare no conflicts of interest.

Acknowledgments

We acknowledge Yang G.M., Li J., PENG Y.X., Wang S.W., Shen B.Y., Li Y.Y., Liu L., Wang C., Xu Y., Lin S.C., Zhang S.W., Tan Y.I., and Zhang F.J. for their participated in this work's literature search, experimental validation, data analysis, and manuscript writing. Zeng X.F., Li Q., and Lu G. supervised the study design and critically read and edited the manuscript. All the authors approved the final version for publication.

Appendix A. Supplementary data

Supplementary data to this article can be found online at <https://doi.org/10.1016/j.jgr.2021.07.005>.

References

- [1] Prakash MD, et al. Methamphetamine: effects on the brain, gut and immune system. *Pharmacol Res* 2017;120:60–7.
- [2] Courtney KE, Ray LA. Methamphetamine: an update on epidemiology, pharmacology, clinical phenomenology, and treatment literature. *Drug Alcohol Depend* 2014;143:11–21.
- [3] Grant KM, et al. Methamphetamine-associated psychosis. *J Neuroimmune Pharmacol* 2012;7(1):113–39.
- [4] Haddar M, et al. Inhibitory effects of Shati/Nat8l overexpression in the medial prefrontal cortex on methamphetamine-induced conditioned place preference in mice. *Addict Biol* 2019.

- [5] Liu Q, et al. Effects of co-administration of ketamine and ethanol on the dopamine system via the cortex-striatum circuitry. *Life Sci* 2017;179:1–8.
- [6] Kohno M, et al. Midbrain functional connectivity and ventral striatal dopamine D2-type receptors: link to impulsivity in methamphetamine users. *Mol Psychiatry* 2016;21(11):1554–60.
- [7] Groenewegen HJ, et al. Organization of the projections from the subiculum to the ventral striatum in the rat. A study using anterograde transport of Phaseolus vulgaris leucoagglutinin. *Neuroscience* 1987;23(1):103–20.
- [8] Jiao D, et al. The role of the GABA system in amphetamine-type stimulant use disorders. *Front Cell Neurosci* 2015;9:162.
- [9] Pereira FC, et al. Disruption of striatal glutamatergic/GABAergic homeostasis following acute methamphetamine in mice. *Neurotoxicol Teratol* 2012;34(5):522–9.
- [10] Kokoshka JM, et al. Methamphetamine treatment rapidly inhibits serotonin, but not glutamate, transporters in rat brain. *Brain Res* 1998;799(1):78–83.
- [11] Pena-Bravo JI, et al. Methamphetamine self-administration elicits sex-related changes in postsynaptic glutamate transmission in the prefrontal cortex. *eNeuro* 2019;6(1).
- [12] Wang B, et al. Methamphetamine modulates the production of interleukin-6 and tumor necrosis factor- α via the cAMP/PKA/CREB signaling pathway in lipopolysaccharide-activated microglia. *Int Immunopharmacol* 2018;56:168–78.
- [13] O'Brien CP, Gardner EL. Critical assessment of how to study addiction and its treatment: human and non-human animal models. *Pharmacol Ther* 2005;108(1):18–58.
- [14] Ricoy UM, Martinez Jr JL. Local hippocampal methamphetamine-induced reinforcement. *Front Behav Neurosci* 2009;3:47.
- [15] Li MH, et al. Amphetamine and methamphetamine increase NMDAR-GluN2B synaptic currents in midbrain dopamine neurons. *Neuropsychopharmacology* 2017;42(7):1539–47.
- [16] Sun L, et al. A selective D3 receptor antagonist YQA14 attenuates methamphetamine-induced behavioral sensitization and conditioned place preference in mice. *Acta Pharmacol Sin* 2016;37(2):157–65.
- [17] Ahmed T, et al. Ginsenoside Rb1 as a neuroprotective agent: a review. *Brain Res Bull* 2016;125:30–43.
- [18] Wang P, et al. Inhibition of autophagy is involved in the protective effects of ginsenoside Rb1 on spinal cord injury. *Cell Mol Neurobiol* 2018;38(3):679–90.
- [19] Jia F, Mou L, Ge H. Protective effects of ginsenoside Rb1 on H2O2-induced oxidative injury in human endothelial cell line (EA.hy926) via miR-210. *Int J Immunopathol Pharmacol* 2019;33. 2058738419866021.
- [20] Li J, et al. Protective effects of ginsenoside Rb1 against blood-brain barrier damage induced by human immunodeficiency virus-1 Tat protein and methamphetamine in sprague-dawley rats. *Am J Chin Med* 2018;46(3):551–66.
- [21] Kim HS, et al. Inhibition by ginsenosides Rb1 and Rg1 of methamphetamine-induced hyperactivity, conditioned place preference and postsynaptic dopamine receptor supersensitivity in mice. *Gen Pharmacol* 1998;30(5):783–9.
- [22] Liao B, Newmark H, Zhou R. Neuroprotective effects of ginseng total saponin and ginsenosides Rb1 and Rg1 on spinal cord neurons in vitro. *Exp Neurol* 2002;173(2):224–34.
- [23] Lu JM, et al. Ginsenoside Rb1 blocks ritonavir-induced oxidative stress and eNOS downregulation through activation of estrogen receptor- β and upregulation of SOD in human endothelial cells. *Int J Mol Sci* 2019;20(2).
- [24] Wu Y, et al. Ginsenoside Rb1 improves leptin sensitivity in the prefrontal cortex in obese mice. *CNS Neurosci Ther* 2018;24(2):98–107.
- [25] Zeng XF, et al. HIV-1 Tat and methamphetamine co-induced oxidative cellular injury is mitigated by N-acetylcysteine amide (NACA) through rectifying mTOR signaling. *Toxicol Lett* 2018;299:159–71.
- [26] Fu K, et al. Pseudoginsenoside-F11 inhibits methamphetamine-induced behaviors by regulating dopaminergic and GABAergic neurons in the nucleus accumbens. *Psychopharmacology (Berl)* 2016;233(5):831–40.
- [27] Alshehri FS, et al. Effects of ceftriaxone on hydrocodone seeking behavior and glial glutamate transporters in P rats. *Behav Brain Res* 2018;347:368–76.
- [28] Yang GM, et al. The potential role of PKA/CREB signaling pathway concerned with gastrin administration on methamphetamine-induced conditioned place preference rats and SH-SY5Y cell line. *Neurotox Res* 2020.
- [29] Barria A, Malinow R. Subunit-specific NMDA receptor trafficking to synapses. *Neuron* 2002;35(2):345–53.
- [30] Brown TE, et al. A silent synapse-based mechanism for cocaine-induced locomotor sensitization. *J Neurosci* 2011;31(22):8163–74.
- [31] Li J, et al. Effect of rhynchophylline on conditioned place preference on expression of NR2B in methamphetamine-dependent mice. *Biochem Biophys Res Commun* 2014;452(3):695–700.
- [32] Tymianski M, et al. Source specificity of early calcium neurotoxicity in cultured embryonic spinal neurons. *J Neurosci* 1993;13(5):2085–104.
- [33] Lin ZY, et al. Ginsenoside Rb1 selectively inhibits the activity of L-type voltage-gated calcium channels in cultured rat hippocampal neurons. *Acta Pharmacol Sin* 2012;33(4):438–44.
- [34] Jiang S, Fang DF, Chen Y. Involvement of N-Methyl-D-Aspartic acid receptor and DL- α -amino-3-hydroxy-5-methyl-4-isoxazole propionic acid receptor in ginsenosides Rb1 and Rb3 against oxygen-glucose deprivation-induced injury in hippocampal slices from rat. *Pharmacology* 2018;101(3–4):133–9.
- [35] Kim S, et al. Inhibitory effect of ginsenosides on NMDA receptor-mediated signals in rat hippocampal neurons. *Biochem Biophys Res Commun* 2002;296(2):247–54.
- [36] Tian X, et al. Developmentally regulated role for Ras-GRFs in coupling NMDA glutamate receptors to Ras, Erk and CREB. *EMBO J* 2004;23(7):1567–75.
- [37] Xing J, Ginty DD, Greenberg ME. Coupling of the RAS-MAPK pathway to gene activation by RSK2, a growth factor-regulated CREB kinase. *Science* 1996;273(5277):959–63.
- [38] De Cesare D, et al. Rsk-2 activity is necessary for epidermal growth factor-induced phosphorylation of CREB protein and transcription of c-fos gene. *Proc Natl Acad Sci U S A* 1998;95(21):12202–7.
- [39] Foulkes NS, Sassone-Corsi P. Transcription factors coupled to the cAMP-signalling pathway. *Biochim Biophys Acta* 1996;1288(3):F101–21.
- [40] West AE, Griffith EC, Greenberg ME. Regulation of transcription factors by neuronal activity. *Nat Rev Neurosci* 2002;3(12):921–31.
- [41] Mehrafza S, et al. Pharmacological evidence for lithium-induced neuroprotection against methamphetamine-induced neurodegeneration via Akt-1/GSK3 and CREB-BDNF signaling pathways. *Iran J Basic Med Sci* 2019;22(8):856–65.
- [42] Carlezon Jr WA, Duman RS, Nestler EJ. The many faces of CREB. *Trends Neurosci* 2005;28(8):436–45.
- [43] Nestler EJ. Historical review: molecular and cellular mechanisms of opiate and cocaine addiction. *Trends Pharmacol Sci* 2004;25(4):210–8.
- [44] Olson VG, et al. Regulation of drug reward by cAMP response element-binding protein: evidence for two functionally distinct subregions of the ventral tegmental area. *J Neurosci* 2005;25(23):5553–62.
- [45] Walters CL, Kuo YC, Blendy JA. Differential distribution of CREB in the mesolimbic dopamine reward pathway. *J Neurochem* 2003;87(5):1237–44.
- [46] Huang M, et al. Thioredoxin-1 downregulation in the nucleus accumbens promotes methamphetamine-primed reinstatement in mice. *Neuropharmacology* 2018;139:117–23.
- [47] Kirschmann EK, et al. Appetitive cue-evoked ERK signaling in the nucleus accumbens requires NMDA and D1 dopamine receptor activation and regulates CREB phosphorylation. *Learn Mem* 2014;21(11):606–15.
- [48] Kim DJ, et al. High concentrations of plasma brain-derived neurotrophic factor in methamphetamine users. *Neurosci Lett* 2005;388(2):112–5.
- [49] Hajheidari S, et al. Effects of prolonged abstinence from METH on the hippocampal BDNF levels, neuronal numbers and apoptosis in methamphetamine-sensitized rats. *Neurosci Lett* 2017;645:80–5.
- [50] Pierce RC, Bari AA. The role of neurotrophic factors in psychostimulant-induced behavioral and neuronal plasticity. *Rev Neurosci* 2001;12(2):95–110.
- [51] Ren W, et al. Time-dependent serum brain-derived neurotrophic factor decline during methamphetamine withdrawal. *Medicine (Baltimore)* 2016;95(5):e2604.
- [52] Grace CE, et al. (+)-Methamphetamine increases corticosterone in plasma and BDNF in brain more than forced swim or isolation in neonatal rats. *Synapse* 2008;62(2):110–21.
- [53] Tian C, Murrin LC, Zheng JC. Mitochondrial fragmentation is involved in methamphetamine-induced cell death in rat hippocampal neural progenitor cells. *PLoS One* 2009;4(5):e5546.
- [54] Thompson PM, et al. Structural abnormalities in the brains of human subjects who use methamphetamine. *J Neurosci* 2004;24(26):6028–36.
- [55] Peterson AB, Abel JM, Lynch WJ. Dose-dependent effects of wheel running on cocaine-seeking and prefrontal cortex Bdnf exon IV expression in rats. *Psychopharmacology (Berl)* 2014;231(7):1305–14.
- [56] Schmidt HD, et al. Epigenetics and psychostimulant addiction. *Cold Spring Harb Perspect Med* 2013;3(3):a012047.